SPACE RESEARCH III

PROCEEDINGS

OF THE THIRD INTERNATIONAL SPACE SCIENCE SYMPOSIUM

WASHINGTON, APRIL 30–MAY 9, 1962

EDITED BY

W. PRIESTER

1963

NORTH-HOLLAND PUBLISHING COMPANY—AMSTERDAM

C2. METEORITES AND TEKTITES

REVIEW OF DIRECT MEASUREMENTS OF INTERPLANETARY DUST FROM SATELLITES AND PROBES

W. M. ALEXANDER, C. W. McCRACKEN, L. SECRETAN and O. E. BERG

Goddard Space Flight Center, National Aeronautics and Space Administration, Greenbelt, Md., USA

26072

Abstract: Direct measurements of selected parameters of interplanetary dust particles have been obtained from experiments on rockets, satellites, and deep space probes. All the available data show excellent agreement when analyzed with respect to the dust particle measurements obtained from Explorer VIII. From this analysis an average cumulative mass distribution curve for dust particles in the vicinity of the earth has been established.

The measured mass distribution presents two predominant features. First, the distribution departs markedly from what is expected from extrapolations of meteor data, and second, the accretion of interplanetary material by the earth is dominated by the small dust particles.

author

Резюме: Непосредственное наблюдение выбранных параметров частиц межпланетной пыли было получено из экспериментов на ракетах, спутниках и пространственных зондах. Все имеющиеся данные прекрасно согласуются, если анализ проводится относительно измерений частиц пыли, полученных с помощью Эксплорера VII. На основании этого анализа была построена кривая распределения средней кумулятивной массы для частиц пыли вблизи от Земли. Измеренное распределение массы обладает двумя основными характеристиками, во-первых, распределение значительно отклоняется от распределения, ожидаемого согласно экстраполляции метеорных данных, во-вторых, в захвате межпланетного материала землей преобладают мелкие частицы пыли.

1. Introduction

An important constituent of the solar system is the cloud of dust surrounding the sun. Knowledge concerning the origin, composition, and dynamic properties of these dust particles is fundamental to considerations of the solar system.

Various techniques have been used in studying the physical and dynamic properties of dust particles in the zodiacal cloud. These include ground-based visual, photographic, and radar meteor observations; photometric observations of the zodiacal light and solar F corona; and various types of collection techniques and laboratory analyses.

From meteor measurements involving observations of individual collisions of meteoroids with the earth's atmosphere, vector velocity, mass, density, and composition have been measured. These studies are limited, in most cases, to particle masses greater than 10^{-4} g. Additional information has been obtained from the collection of remnants of meteoroidal and dust particle material which have survived passage through the atmosphere. Composition, age, and gross accretion rates were determined from these analyses. Zodiacal light observations represent the only ground-based technique which has been used to obtain measurements of the sizes and dynamics of dust particles in interplanetary space with masses less than 10^{-6} g.

Another technique for measuring physical and dynamic properties of dust particles became a reality with the advent of vehicles capable of placing experiments in space. Detectors have been developed which are capable of measurements on individual dust particles with masses as small as 10^{-13} g. The dust particle measurements in space started with experiments on sounding rockets in 1949. Since the successful launching of Explorer I (1958 Alpha), results have been obtained from experiments on fourteen United States and Soviet Union satellites and space probes. Six different types of sensors have been used to measure the following particle parameters: momentum, kinetic energy, penetration, and fracture properties. The results of these rocket and satellite measurements are presented in the following sections.

2. Direct measurements from microphone systems

The microphone type of dust particle sensor has basically consisted of a piezoelectric crystal microphone attached to a metallic sounding board. The electrical signal that is generated when an impacting dust particle delivers a mechanical impulse to the sounding board is amplified and pulse-height analyzed in order to obtain information about the particle. Analog calibrations, performed in the laboratory by dropping carefully selected glass spheres onto the sounding boards, have consistently shown (for low velocities) that the microphone system is sensitive to the momentum of an impacting particle. Hypervelocity studies with microparticles from shaped charges [1] tend to confirm the momentum sensitivity. Use of the theoretical results of Stanyukovich [2] lead to an energy sensitivity, while the use of those of Lavrentyev [3] give still a different dependence on the particle velocity.

The direct measurements can be expressed in terms of the particle mass, subject only to minor uncertainties. These uncertainties include the choice of a proper average speed (relative to the satellite) for the particles; the

determination of an effective coefficient of restitution for hypervelocity microparticle impacts; and the computation of the appropriate correction factors for shielding by the earth, for the solid viewing angle of the sensor, and for the orientation of the solid viewing angle relative to the apex of the earth's motion. The various correction factors have been chosen such that the minor corrections that will most probably become necessary will leave the results of this analysis essentially unchanged.

Microphone systems have provided the greatest quantity of information about the interplanetary dust particles. These systems have flown on more vehicles and over a greater range of geocentric distances than any of the other systems. In addition, they are more nearly calibrated than other types of dust particle sensors. It will be assumed, for the purposes of the present analysis, that the microphone systems are momentum sensitive and that the ratio of the mechanical impulse to the impact-momentum of a particle is unity. A small correction, estimated to be a factor of 2 or 3, can be introduced later when hypervelocity laboratory studies are completed.

The microphone system on Explorer VIII (1960 Xi) utilized two metallic sounding boards attached to a conical section of the spin-stabilized satellite. The solid viewing angle of the system was 2π sr and remained almost centered on the antapex of the earth's motion during the lifetime of the experiment. From an analog calibration performed in the laboratory, the limiting sensitivities for the three ranges of sensitivity were found to be 2.5×10^{-3} 2.5×10^{-2}, and 2.5×10^{-1} dyne seconds. These may be expressed in terms of particle mass as 1.0×10^{-9}, 1.0×10^{-8}, and 1.0×10^{-7} g, respectively, if an average speed (relative to the satellite) of 25 km sec^{-1} is assumed. The large separations of the limiting sensitivities used in the microphone system on Explorer VIII are of particular importance in view of the excellent data sample that was obtained. The magnitude of the total range of sensitivity allows not only a definition of the influx rates within the three ranges but also the establishment of the shape of a segment of an average mass distribution curve.

The fine structure in the influx rate measured with the microphone system on Explorer VIII is presently being analyzed. The large variations (at least plus or minus an order of magnitude from the mean within intervals of only a few hours for dust particles with masses of about 10^{-9} g) are being studied to determine their physical significance. The preliminary readouts of the total numbers of impacts used in establishing the average mass distribution curves that were reported earlier [4, 5] have been confirmed. Exact specification of these numbers awaits completion of the analyses that are in progress, but "revised preliminary "numbers may be given. They are:

3726 dust particles with momenta equal to or greater than 2.5×10^{-3} dyne seconds, 76 with momenta equal to or greater than 2.5×10^{-2} dyne seconds, and 1 or 2 with momenta equal to or greater than 2.5×10^{-1} dyne seconds. The corresponding limits on particle mass were given in an earlier paragraph. The exposed area of the sounding boards was 7.0×10^{-2} m^2, and the lifetime of the experiment was 3.47×10^6 seconds.

A correction factor of 2 is applied in order to convert the influx rates to omnidirectional values before the data are plotted as the cumulative mass distribution curve shown in fig. 1. Although the data point for the scale of lowest sensitivity is not very significant. it lies on the straight line segment indicated by the two data points that are significant. The equation of a straight line segment that very nearly fits the data points shown in fig. 1 is:

$$\log I = -17.0 - 1.70 \log m, \tag{1}$$

in which I is the omnidirectional influx rate in particles m^{-2} sec^{-1}, and m is the particle mass in grams.

The spacecraft from which direct measurements with microphone systems have been obtained in the United States are listed, together with the relevant data, in table 1. Average particle speeds of 30 km sec^{-1} have been used for the omnidirectional sensors and for sensors mounted on spinning or tumbling

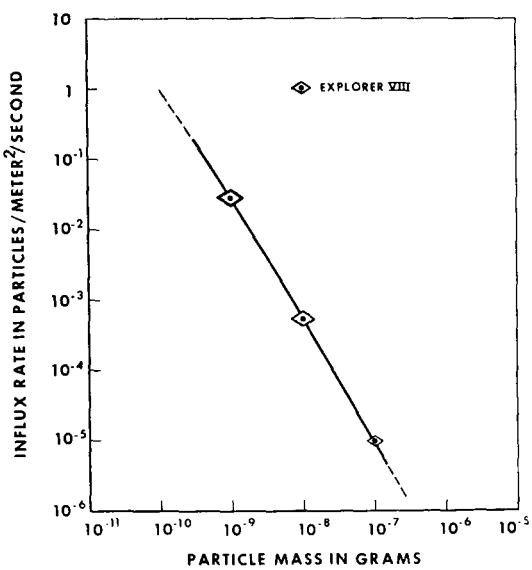

Fig. 1. Cumulative mass distribution established by the microphone system on Explorer VIII.

TABLE 1

Direct measurements obtained with microphone systems on United States satellites and space probes.

Spacecraft	Momentum sensitivity (dyne seconds)	Mass sensitivity (grams)	Effective area (meter^2)	Exposure time (seconds)	Exposure (m^2 sec)	Number of particles	Cumulative influx rate (particles/m^2/sec)	
							Observed	Corrected
Explorer VIII	2.5×10^{-3}—2.5×10^{-2} 2.5×10^{-2}—2.5×10^{-1} $>2.5\times10^{-1}$	1.0×10^{-9}—1.0×10^{-8} 1.0×10^{-8}—1.0×10^{-7} $>1.0\times10^{-7}$	7.0×10^{-2}	3.5×10^{6}	2.4×10^{5}	$\sim$3650 $\sim$75 1 or 2	1.5×10^{-2} 3.1×10^{-4} $\sim5.0\times10^{-6}$	3.0×10^{-2} 6.2×10^{-4} $\sim1.0\times10^{-5}$
Vanguard III	$>1.0\times10^{-2}$	$>3.3\times10^{-9}$	4.0×10^{-1}	6.9×10^{6}	2.8×10^{6}	$\sim$3500	1.3×10^{-3}	2.0×10^{-3}
Explorer I	$>2.5\times10^{-3}$	$>8.3\times10^{-10}$	2.3×10^{-1}	7.9×10^{4}	1.8×10^{4}	145	8.4×10^{-3}	1.7×10^{-2}
Pioneer I	$>1.5\times10^{-4}$	$>5.0\times10^{-11}$	3.9×10^{-2}	1.1×10^{5}	4.2×10^{3}	17	4.0×10^{-3}	1.6×10^{-2}
Ranger I	$>3.0\times10^{-5}$	$>1.0\times10^{-11}$	8.0×10^{-4}	1.1×10^{4}	8.8	64	7.3	4.0×10
Midas II	$>3\times10^{-4}$	$>1\times10^{-10}$	6.9×10^{-2}	4.0×10^{3}	2.7×10^{2}	67	2.5×10^{-1}	5.0×10^{-1}
Samos II	$\gtrsim3\times10^{-4}$	$\gtrsim1\times10^{-10}$	6.9×10^{-2}	?	?	?	3.4×10^{-1}	6.8×10^{-1}
SLV-1	$\gtrsim9\times10^{-3}$	$\gtrsim3\times10^{-9}$	8.0×10^{-1}	9.5×10^{2}	7.6×10^{2}	10	1.3×10^{-2}	2.6×10^{-2}

vehicles that viewed most of the celestial sphere. An attempt has been made to apply correction factors for shielding by the earth and lack of omnidirectionality of the sensors. All data were converted to omnidirectional influx rates.

Reading of the telemetered data from Vanguard III (1959 Eta) has now been completed and is in the final stages of analysis. More than 6000 impacts were recorded during the 80 day lifetime of the experiment. Of this number, approximately 2800 impacts occurred in a 70 hour interval on 16–18 November, which was coincident in time with the expected annual return of the Leonid meteor shower. An average influx rate has been computed from the Vanguard III data on the basis of approximately 3500 impacts. A factor of 1.5 was used to correct for shielding by the earth.

The data given for Explorer I (1958 Alpha) and Pioneer I are those reported by Dubin [6, 7]. The total number of impacts (145) for Explorer I was used in computing an average influx rate even though more than one-half of the impacts probably represented an interplanetary dust particle event [8, 9]. The high influx rates during the dust particle event were somewhat counteracted by an interval of low rates, so an influx rate computed from the total number of impacts serves very well in the present analysis. A factor of 2 was used in correcting for shielding by the earth and in allowing for the fact that the sensor was not completely omnidirectional. The microphone system on Pioneer I registered 25 impacts, of which 17 are considered to represent impacting dust particles. No correction for shielding by the earth was made, because Pioneer I spent most of its time at large geocentric distances (2 to 19 earth radii). A factor of 4 was used in converting to an omnidirectional influx rate.

A preliminary readout of the data from the microphone and coated photomultiplier systems on Ranger I has been reported by Alexander and Berg [10]. In this system, the two sensors were capable of operating in coincidence as well as independently. The data for the microphone system alone are given in table 1.

The results from the microphone system on Midas II (1960 Zeta 1) and preliminary results from a similar system on Samos II (1961 Alpha 1) have been reported by Soberman and Della Lucca [11]. The data were obtained, as in the case of Explorer I, in real time as the satellite passed over telemetry stations.

The data from a microphone system on SLV-1 (a Vanguard satellite that failed to achieve orbit) have been reported by LaGow, Schaefer, and Schaffert [12]. A data point that is of use in the present analysis can be obtained if the sensitivity of the system is recomputed on the basis of momentum

rather than energy. The bursts of counts observed were most likely produced when the expended third stage motor sputtered and bumped the palyoad [13]. Therefore, only 10 of the 17 impacts are used in computing an influx rate. The value of the mass sensitivity assigned to this system has been computed from calibration data that were given [12].

Some of the earliest direct measurements that were of quantitative value were obtained with microphone systems on a series of seven successful high altitude rockets instrumented and flown by Oklahoma State University [5, 14. 15]. The data from these rockets are summarized in table 2. Average particle speeds have been assigned for each sensor of each rocket until the distribution of orbits of dust particles can be determined. Most of the sensors

TABLE 2

Direct measurements obtained with microphone systems on the O.S.U. rockets.

Rocket	Momentum sensitivity (dyne sec)	Particle speed (km/sec)	Mass sensitivity (grams)	Number of impacts	Exposure $h>110$ km (m^2 sec)	Cumulative influx rate (particles/m^2/sec)
Aerobee No. 80	$>6.0\times10^{-4}$	70	$>8.6\times10^{-11}$	49	5.0	9.8
	$>3.0\times10^{-3}$	70	$>4.3\times10^{-10}$	10	5.0	2.0
	$>1.0\times10^{-3}$	40	$>2.5\times10^{-10}$	3	50	6.0×10^{-2}
	$>3.0\times10^{-3}$	40	$>7.5\times10^{-10}$	1	50	2.0×10^{-2}
Aerobee No. 88	$>1.3\times10^{-4}$	20	$>6.5\times10^{-11}$	6	3.0	2.0
	$>2.0\times10^{-3}$	20	$>1.0\times10^{-9}$	1	3.0	3.3×10^{-1}
	$>4.7\times10^{-4}$	35	$>1.3\times10^{-10}$	17	30	5.7×10^{-1}
	$>1.0\times10^{-3}$	35	$>2.9\times10^{-10}$	7	30	2.3×10^{-1}
Nike-Cajun AF-2	$>6.0\times10^{-4}$	40	$>1.5\times10^{-10}$	45	31	1.5
	$>1.2\times10^{-3}$		$>3.0\times10^{-10}$	15		4.8×10^{-1}
	$>4.0\times10^{-3}$		$>1.0\times10^{-9}$	3		9.7×10^{-2}
Nike-Cajun AA6.203	$>3.0\times10^{-4}$	35	$>8.6\times10^{-11}$	55	37	1.5
	$>3.0\times10^{-3}$		$>8.6\times10^{-10}$	3		8.1×10^{-2}
Nike-Cajun AA6.204	$>7.0\times10^{-4}$	40	$>1.8\times10^{-10}$	32	33	9.7×10^{-1}
	$>3.0\times10^{-3}$		$>7.5\times10^{-10}$	1		3.0×10^{-2}
Nike-Cajun AA6.206	$>1.5\times10^{-4}$	35	$>4.3\times10^{-11}$	12	24	5.0×10^{-1}
	$>1.0\times10^{-3}$		$>2.9\times10^{-10}$	1		4.2×10^{-2}
	$>7.0\times10^{-4}$		$>2.0\times10^{-10}$	6		2.5×10^{-1}
Spaerobee 10.01	$>5.0\times10^{-4}$	60	$>8.3\times10^{-11}$	20	8.1	2.5

on the rockets were exposed to the high speed component of dust particle influx.

The direct measurements obtained with microphone systems on rockets, satellites, and spacecraft of the Soviet Union have been reported by Nazarova [16, 17] and are summarized in table 3. Some of the quantities in table 3 have been computed on the basis of information given by Nazarova in order that data from the U.S. and U.S.S.R. space vehicles can be included in the same analysis.

The sensitivities for the microphone systems on the Soviet spacecraft were expressed by Nazarova in terms of particle mass. The microphone system was assumed to be energy sensitive, and an average particle speed of 40 km sec^{-1} was assumed for the satellites and space probes in converting to particle mass. An average particle speed of 40 km sec^{-1} was used in an early analysis by McCracken [14], but this value is now regarded as being too high. A value of 30 km sec^{-1} seems more reasonable and will be used until information on the velocity distribution of the dust particles has been obtained. The mass sensitivities for the microphone systems on the Soviet spacecraft are therefore reduced by the square of the ratio of 40 to 30 in order to compensate for the difference in the assigned particle speeds. The average particle speed assumed in computing the mass sensitivities of the microphone systems on the geophysical rockets was 15 km sec^{-1}, so the mass sensitivities given by Nazarova are increased by a factor of 4 when converting to 30 km sec^{-1}.

The influx rates measured by Sputnik III (1958 Delta 2) underwent tremendous changes during the first three days of operation of the equipment. The influx rates, as reported by Nazarova [16, 18], were 4 to 11 particles m^{-2} sec^{-1} on 15 May (day of launch), 5×10^{-4} particles m^{-2} sec^{-1} on 16–17 May, and less than 10^{-4} particles m^{-2} sec^{-1} during the interval 18–26 May. Nazarova attributes the high influx rates during the first few days to a meteoroid shower, but her conclusion is open to question. In any case, only the influx rate given for the last 9 days of operation can be used in establishing an average mass distribution curve. It is not clear whether Nazarova corrected the influx rate from Sputnik III for shielding by the earth, so the influx rate is left in table 3 as it was given.

The method of encoding information into the telemetered signal on Lunik I was such that only very crude upper limits to the influx rates can be specified. Only that influx rate measured by the scale of highest sensitivity is of any value in the present analysis. Lunik I, Lunik II, and the Interplanetary Station (1959 Theta) operated at large geocentric distances, obviating corrections for shielding by the earth. No attempt has been made to correct the influx rates from the three geophysical rockets to omnidirectional values

TABLE 3

Direct measurements obtained with microphone systems on the Soviet Union rockets, satellites, and space probes.

Vehicle	Mass sensitivity (grams)		Effective area (meter²)	Exposure time (seconds)	Exposure (m² sec)	Number of particles	Influx rate (particles/m²/sec)	
	$v = 40$ km/sec	$v = 30$ km/sec					(Nazarova)	Cumulative
Sputnik III	$8.0\times10^{-9}-2.7\times10^{-8}$ $2.7\times10^{-8}-1.5\times10^{-7}$ $1.5\times10^{-7}-5.6\times10^{-6}$ $>5.6\times10^{-6}$	$1.4\times10^{-8}-4.8\times10^{-8}$ $4.8\times10^{-8}-2.7\times10^{-7}$ $2.7\times10^{-7}-1.0\times10^{-5}$ $>1.0\times10^{-5}$	0.34	$\sim8\times10^{5}$	3×10^{5}	?	(see text)	$<1\times10^{-4}$
Lunik I	$2.5\times10^{-9}-1.5\times10^{-8}$ $1.5\times10^{-8}-2.0\times10^{-7}$ $>2.0\times10^{-7}$	$4.4\times10^{-9}-2.7\times10^{-8}$ $2.7\times10^{-8}-3.6\times10^{-7}$ $>3.6\times10^{-7}$	0.2	3.6×10^{4}	7.2×10^{3}	<16 <4 <1	$<2\times10^{-3}$ $<5\times10^{-4}$ $<1\times10^{-4}$	$<2.9\times10^{-3}$ $<7.0\times10^{-4}$ $<1.4\times10^{-4}$
Lunik II	$2.0\times10^{-9}-6.0\times10^{-9}$ $6.0\times10^{-9}-1.5\times10^{-8}$ $>1.5\times10^{-8}$	$3.6\times10^{-9}-1.1\times10^{-8}$ $1.1\times10^{-8}-2.7\times10^{-8}$ $>2.7\times10^{-8}$	0.2	1.1×10^{5}	2.2×10^{4}	0 0 2	$<5\times10^{-5}$ $<5\times10^{-5}$ 9×10^{-5}	 9.1×10^{-5}
Interplanetary station	$1.0\times10^{-9}-3.0\times10^{-9}$ $3.0\times10^{-9}-8.0\times10^{-9}$ $>8.0\times10^{-9}$	$1.8\times10^{-9}-5.3\times10^{-9}$ $5.3\times10^{-9}-1.4\times10^{-8}$ $>1.4\times10^{-8}$	0.1	2.3×10^{4}	2.3×10^{3}	1 5 1	4×10^{-4} 2×10^{-3} 4×10^{-4}	3.0×10^{-3} 2.6×10^{-3} 4.3×10^{-4}
Geoph. Rocket I	—	$\gtrsim2.5\times10^{-9}$	4	1.3×10^{2}	5.4×10^{2}	?	6×10^{-2}	6×10^{-2}
Geoph. Rocket II	—	$\gtrsim2.5\times10^{-9}$	4	1.5×10^{2}	5.9×10^{2}	?	5×10^{-2}	5×10^{-2}
Geoph. Rocket III	—	$\gtrsim2.5\times10^{-9}$	4	8.5×10	3.4×10^{2}	?	7.5×10^{-1}	7.5×10^{-1}

because the orientations of the rockets and solid viewing angles of the sensors have not been reported.

3. Direct measurements from photomultiplier and rocket collection systems

Experiments which measured the kinetic energies of micron-size dust particles were flown on three rockets [9, 19, 20] and two satellites [9, 10]. The sensors measured the intensity of the visible light emitted during each impact of a microparticle with a speed greater than 5 km sec^{-1}. Light emitted from impacts of micron-size particles with speeds between 4 and 11 km sec^{-1} has been observed in laboratory studies [21]. Measurements of the intensity and duration of the light flash provide a means for determining the kinetic energy of an impacting particle. Results of the laboratory studies indicate that the light flash sensor detected particles with masses greater than 10^{-13} g.

The configuration of the sensors in each of the five experiments was different, but the principle of light flash detection was the same. The basic detector unit was a photomultiplier tube. The surface exposed to impacts in the experiments was Lucite [19, 20] and glass [9, 10]. A few thousand angstroms of aluminium were evaporated on the impact surface to shield the photocathode from background light. When a dust particle penetrated the aluminium during an impact, light from the impact flash could reach the photocathode. The rocket experiments exposed larger impact areas than the satellite instrumentation to compensate for the shorter exposure times of the rocket flights. The impact surface for each of the two satellite detectors was the face of an end-on-type photomultiplier tube. An intensive effort

TABLE 4

Direct measurements from photomultiplier systems on United States rockets and satellites

	Half-angle of detector cone of vision	Exposure (m^2 sec)	Number of particles	Influx rate (particles/m^2/sec)	Omni-directional influx rate
Aerobee NRL 25	80°	0.63	101	160	390
Jupiter AM–28	80°	2.2	4	1.63	4
Explorer VIII (preliminary)	60°	4.3	110	25	200
Ranger I (preliminary)	75°	8.5	179	21	114

was made to make the sensors insensitive to Cerenkov radiation and to energetic particles.

The results of the light flash detector measurements are given in table 4. The cone of vision of a detector, the exposure, and the total number of impacts are given for each measurement. An impact rate is computed and then normalized to 4π sr. (These computations also include correction factors for earth shielding.)

Aerobee NRL–25 was launched at 02 00 hours local time. Thus, the light flash detector was exposed to the high speed component of the dust particle influx. The Jupiter AM–28 rocket was launched at 19 00 hours local time, so the detector was exposed to the low speed component of the influx. For purposes of comparison, the rocket results are normalized to a speed of 30 km sec^{-1}. A speed of 45 km sec^{-1} is used as the average speed of the dust particles to which the Aerobee NRL–25 sensor was exposed. Since the detector sensitivity is a function of the square of the particle speed, the influx rate of 390 particles m^{-2} sec^{-1} is reduced to 173 particles m^{-2} sec^{-1} in order to obtain an omnidirectional influx at an average speed of 30 km sec^{-1} (a linear relationship is assumed between influx rates and mass sensitivity). A similar computation is made for the Jupiter AM–28 measurement using a value of 12 km sec^{-1} for the average dust particle speed. The omnidirectional influx rate for this experiment becomes 25 particles m^{-2} sec^{-1}.

The Skylark rocket flown by Lovering [21] contained a light flash experiment very similar to that on Aerobee NRL–25. No events were observed, but because of the following reasons there is a possibility that the experiment did not survive launch. The sensor was a 1P21 photomultiplier, and the rocket was a Skylark, which has a solid propellant motor. The system was subjected to 70 g acceleration test in a centrifuge. A meaningful environmental qualification test should have also included severe shock and vibration tests, since the 1P21 is not ruggedized. An in-flight sensor calibration using a light source would have verified the launch survival of the detector. The Jupiter AM–28 experiment and both satellite experiments contained this feature in the experiment instrumentation.

The measurements from the satellites are corrected for earth shielding and normalized to 4π sr. The data from the Explorer VIII and Ranger I experiments are restricted to satellite nighttime measurements in order to eliminate any extraneous counts caused by sunlight. The average omnidirectional influx rates for the Explorer VIII and Ranger I measurements are 200 and 114 particles m^{-2} sec^{-1}, respectively, for particles with masses of 10^{-13} g and greater.

Another estimate of the influx rates for dust particles somewhat smaller

than those covered by the direct measurements obtained with microphone systems has been reported by Soberman, Hemenway, *et al.* [22]. A recoverable high-altitude rocket was used in obtaining a remarkable collection of particles at altitudes greater than 88 km. An influx rate of 300 particles m^{-2} sec^{-1} was estimated for the particles with diameters equal to or greater than 3 μ. The cumulative influx rate plotted as a function of particle diameter has a negative slope of 1.3 and applies to particles with diameters as small as 0.2 μ. If a mass density of 3 g cm^{-3} is used [22], the influx rates estimated from this collection may be compared to those obtained from the other direct measurements. No shielding corrections are introduced, since the collectors faced in the general direction of the apex of the earth's motion.

4. Cumulative mass distribution curve from direct measurements

The direct measurements obtained with the microphone, photomultiplier, and rocket collection systems are plotted as a cumulative mass distribution curve in fig. 2. Two characteristics of the data used in establishing the curve should be emphasized. First, the influx rates are expressed as omnidirectional values, and secondly, the curve is the result of a series of experiments in the vicinity of the earth. How well the curve applies to other regions of space is not presently known.

All of the microphone data for the mass range of 10^{-10} g to 10^{-7} g are compared, in fig. 2, to the Explorer VIII results (presented in fig. 1). A study of the data points in fig. 2 demonstrates the degree of consistency with which the average influx rates derived from all microphone measurements fit the curve.

The photomultiplier results allow an extension, to approximately 10^{-13} g, of the distribution curve obtained with microphone systems. The reported influx rates from the rocket collection experiment [22] are somewhat higher than the photomultiplier detector results. However, the 80 to 150 km altitude range of the collection experiment probably contains an abundance of decelerated microparticles. This is an explanation for the high spatial density of micron-size particles reported from the collection results.

The cumulative mass distribution curve is not a constant mass to magnitude curve, and the slope appears to change rapidly with decreasing particle size. The radiation pressure cut-offs as a function of the mass density are also shown in fig. 2. On a cumulative mass distribution curve, the slope of the curve should approach zero as the radiation pressure limits are reached. The results for particles with masses between 10^{-13} g and 10^{-10} g represent initial measurements which are inherently more uncertain than the micro-

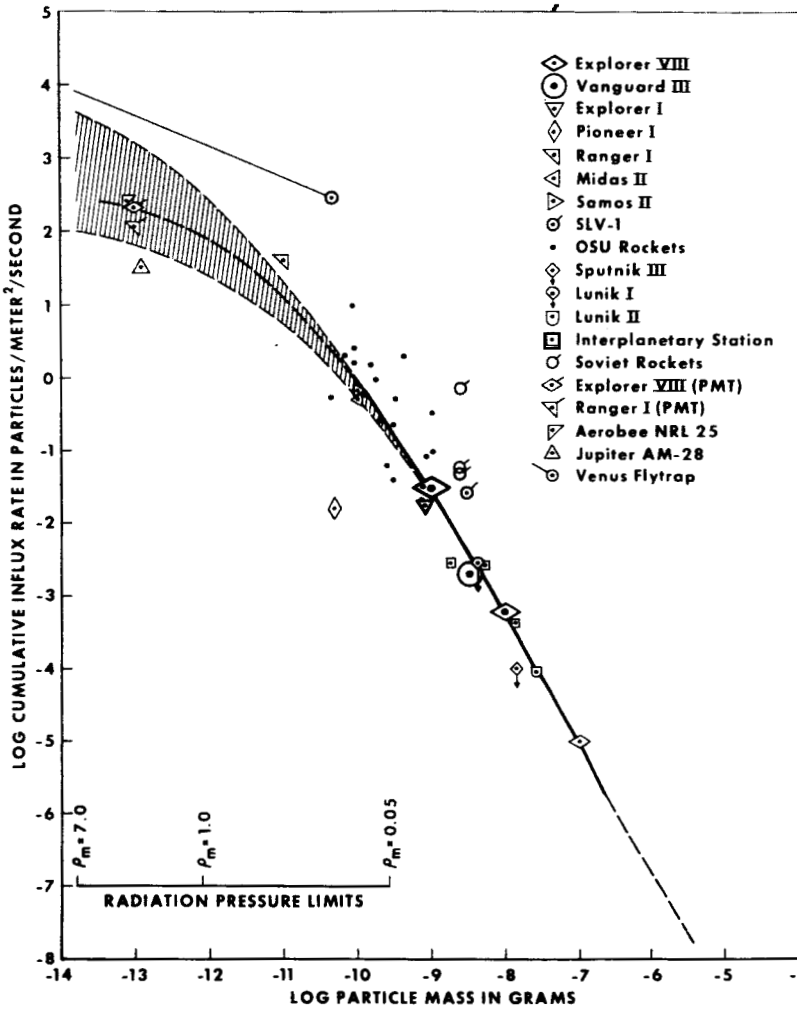

Fig. 2. An average cumulative mass distribution curve for the vicinity of earth derived from all the available direct measurements obtained with microphone and photomultiplier systems.

phone data. As the number and sophistication of measurements increase for this range of particle size, the mechanisms controlling the distributions of these micron-size dust particles will be better understood.

5. Results from penetration and fracture experiments

Thirteen experiments with penetration or fracture types of dust particle sensors have been flown on seven U.S. satellites. In all but two cases, the

numbers of events detected by these sensors were one or zero; therefore, a significant average influx rate for dust particles cannot be determined. A comparison can, however, be made between the results of these experiments and the average mass distribution curve (fig. 3) established from measurements with microphone systems.

The fracture type sensors consisted of continuous wire wrapped around an insulating support material. An impact event was observed when a colliding dust particle fractured the wire and caused an open circuit. Manring

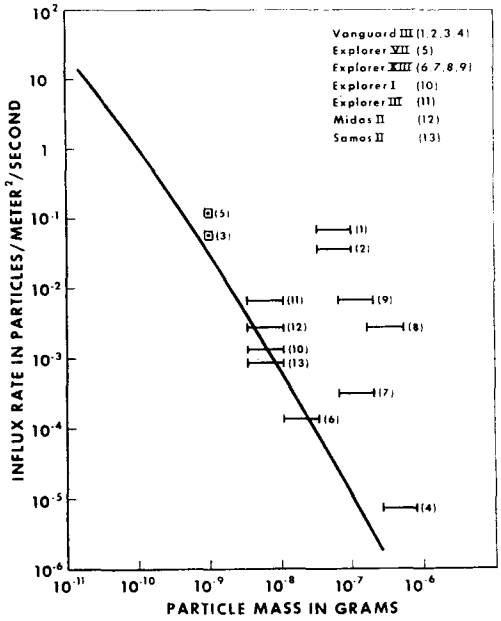

Fig. 3. Average influx rates computed (on the basis of a probability of 0.99 of at least one impact) from penetration and fracture experiments and compared with those given by the cumulative mass distribution curve.

[23] (Explorer I and III), Soberman and Della Lucca [11] (Midas II and Samos II), and Secretan (Explorer XIII) have flown the wire grid type sensor on five satellites. The major differences among these sensors were the wire size and total exposed area. The mass of the dust particle which would fracture the wire is taken here as being comparable to that reported by Manring [23] and Cohen, *et al.* [24].

Four different types of penetration experiments have been flown on three satellites. Three of the sensors required a perforation of the exposed surface, and one sensor required a crater with a diameter sufficient to destroy the

sensing element. LaGow and Secretan [25, 26] developed three of these sensors for Vanguard III. The first type of sensor consisted of a strip of chromium, 300 μ wide and 1 μ to 3 μ deep, evaporated on Pyrex glass. The resistance of the strip was monitored, and a complete break of the chromium was required in order to register an impact. The threshold sensitivity in terms of particle mass was determined by computing the diameter of the crater necessary to produce an open circuit. The second type of sensor consisted of two hermetically sealed and pressurized zones. The exposed surface of the zones was 0.162 m^2 of the 26 mil magnesium skin of the satellite. A differential pressure transducer constantly monitored the pressure between the two zones, so that a puncture of either or both zones could be detected. The third sensor consisted of a CdS cell covered by a $\frac{1}{4}$ mil mylar film which was made opaque by evaporating aluminum on both sides of the film. As punctures occurred, the admitted sunlight changed the resistance of the CdS cell allowing the effective hole size to be measured. More than one puncture could have been observed with this sensor. This experiment was also flown on Explorer VII.

Davison [27, 28] has flown the fourth type of penetration experiment on Explorer XIII. A plate of stainless steel was mounted in front of a foil gage consisting of a continuous path of gold deposited on silicone rubber. The foil gage was separated from the metallic plate by a mylar insulator. Two thicknesses of stainless steel, 75 μ and 150 μ, were used. A particle penetrating the metal would also have fractured the gold foil, causing an open circuit and detection of an impact.

Using $\frac{1}{4}$ mil mylar film and micron-size particles with velocities as high as 11 km/sec, Friichtenicht [21] has found that the diameter of the hole is 1.5 $\pm$ 0.5 times the diameter of the impacting particle for velocities greater than 3.5 km sec^{-1}. Secretan and Berg (unreported results), using the same accelerator, have found no marked deviation from the above studies. These results are the basis for the calibration used in the interpretation of the mylar film-CdS experiment. The other three penetration sensors (magnesium and stainless steel) required a perforation or a crater. An extensive series of penetration experiments has been performed by Summers, *et al.* [29, 30]. The penetration equation developed in these studies was used to compute, for these three sensors, the threshold sensitivity in terms of particle mass.

The pertinent information concerning the penetration and fracture experiments are presented in table 5. The exposure (area-time product) includes a consideration of earth shielding, except for the two measurements by Soberman and Della Lucca [11]. The influx rates for Explorer III (2 impacts) and Samos II (8 impacts) were computed [23, 11] from the number

TABLE 5

Direct measurements from penetration and fracture experiments on United States satellites

Satellite	Type of dust particle sensor	Critical dimension for penetration or fracture	Range of threshold particle mass (gm)	Exposure (corrected) (m^2 sec)	Number of particles	Predicted influx rate $P_1 = 0.99$ (particles/m^2/sec)	Data point shown in fig. 3
Vanguard III	Pyrex-Chromium strip	300 μ	$4.0\times10^{-8}-1.2\times10^{-7}$	7.0×10^{1}	0	6.2×10^{-2}	1
	Pyrex-Chromium strip	300 μ	$4.0\times10^{-8}-1.2\times10^{-7}$	1.4×10^{2}	0	3.3×10^{-2}	2
	Mylar – CdS cell	1/4 mil	1.2×10^{-9}	8.7×10^{1}	0	5.3×10^{-2}	3
	Magnesium zones	26 mil	$3.0\times10^{-7}-9.0\times10^{-7}$	7.2×10^{5}	0	6.4×10^{-6}	4
Explorer VII	Mylar – CdS cell	1/4 mil	1.2×10^{-9}	3.9×10^{1}	1	1.2×10^{-1}	5
Explorer XIII	Stainless steel	75 μ	$1.1\times10^{-8}-3.3\times10^{-8}$	3.4×10^{4}	0	1.4×10^{-4}	6
	Stainless steel	150 μ	$8.8\times10^{-8}-2.6\times10^{-7}$	8.5×10^{3}	0	5.6×10^{-4}	7
	Wire grids	75 μ	$2.0\times10^{-7}-6.0\times10^{-7}$	1.7×10^{3}	0	2.7×10^{-3}	8
	Wire grids	50 μ	$6.7\times10^{-8}-1.8\times10^{-7}$	7.7×10^{2}	0	6.0×10^{-3}	9
Explorer I	Wire grids	17 μ	$4.2\times10^{-9}-1.2\times10^{-8}$	3.6×10^{3}	0	1.3×10^{-3}	10
Explorer III	Wire grids	17 μ	$4.2\times10^{-9}-1.2\times10^{-8}$	2.4×10^{2}	2	6.4×10^{-3}	11
Midas II	Wire grids	20 μ	$4.2\times10^{-9}-1.5\times10^{-8}$	2.0×10^{3}	0	2.3×10^{-3}	12
Samos II	Wire grids	20 μ	$4.2\times10^{-9}-1.5\times10^{-8}$	1.1×10^{4}	8	8.0×10^{-4}	13

of events and the corresponding exposures. One event was observed on Explorer VII and no events were observed on ten of the remaining experiments.

For these eleven experiments with 0 or 1 events, a meaningful rate cannot be found by the simple computation indicated in the above paragraph. The probability of at least one impact on an experiment with a given area and exposure time can be found by assuming Poisson statistics, which leads to the following equation:

$$P_1 = 1 - e^{-\gamma}, \text{ where}$$

P_1 = probability of at least one hit,
γ = atr,
at = exposure (m^2 sec), and
r = average influx rate (particles/m^2/sec).

Letting $P_1 = 0.99$, an average influx rate, r, can be computed. This becomes the average influx rate which predicts at least one event with a probability of 0.99 for a given particle mass.

If these influx rates are compared to the mass distribution curve of fig. 2, there are three possible positions of r in relation to the curve (at a given mass sensitivity). The first position is above the curve, implying that a rate greater than the one predicted by the curve is necessary for at least one event *or* that the exposure was insufficient. The second position is on the curve, implying that the experiment should have had at least one event. The third position is below the curve, implying that the exposure was sufficient to expect at least one hit or that the predicted rate could be lower than the one of the curve in order to expect at least one hit.

The uncertainties indicated in fig. 3 represent a consideration of the major variations known at the present time concerning the parameters (particle velocity and density) involved in hypervelocity impacts. The data show that some of the experiments did not have sufficient exposure to yield significant information. Within the uncertainties shown, the measurements do support the average mass distribution curve previously presented, especially within the mass range of 10^{-8} g to 10^{-6} g. The curve shown in fig. 3 predicts the wire grid fractures that occurred on Explorer III [23] and Samos II [11] and the survival (without puncture) of the penetration experiments on Vanguard III [25] and Explorer XIII [27].

The analysis of all of the direct measurements has shown no significant departures from the average mass distribution curve that was derived from the microphone experiment on Explorer VIII. Now that it has been demonstrated that the direct measurements are self-consistent, comparisons of the

direct measurements with results obtained by other observational techniques can be attempted. Information that deserves special attention in such a comparison comes from the observations of meteors, zodiacal light, and the solar F corona.

6. Comparison of direct measurements with results from observations of meteors

Extrapolating the results from meteor observations toward smaller particles represented a major method of estimating influx rates for dust particles before the advent of the direct measurement technique. The tabulation by Watson [31] of influx rates of meteors followed the constant mass per magnitude relationship, rendering the extrapolation to smaller particles relatively easy. Such extrapolations have been made in the past, with the most commonly used ones being those of Grimminger [32] and Whipple [33].

Even the earliest of the rockets in the OSU series [14] gave influx rates several orders of magnitude higher than was expected on the basis of the extrapolations of meteor data. Meanwhile, the observation of coasting in the train of a double station photographic meteor led to the hypothesis of a very low value of mass density ($\varrho_m = 0.05$ g cm^{-3}) for meteoroids [34]. Whipple [35] (using this low value of mass density together with the corresponding change in the mass to magnitude relationship, the influx rates reported by Millman and Burland [36], and an average speed of 28 km sec^{-1} for the meteoroids) proposed a constant mass per magnitude extrapolation. This new distribution, showing much higher influx rates than shown by the Watson distribution for particles of a given mass, did not agree with the early direct measurements.

The results of Millman and Burland [36] and of Hawkins and Upton [37] showed that the constant mass per magnitude relationship was not valid, even for the meteoroids. If the distribution curve given by Hawkins and Upton had been extrapolated into the direct measurements range of particle mass, it would have shown some degree of compatibility with the early results from the OSU rockets. Such an extrapolation was not in agreement with the direct measurements that were available from the early satellites [38, 39].

It was on the basis of this early evidence for disagreement between the direct measurements and the extrapolated meteor results that McCracken and Alexander first suggested that a constant mass per magnitude law did not apply in the direct measurements range of particle mass [14]. The direct measurements available at that time were not sufficient to confirm this

hypothesis, nor did sufficient data become available until the results from Explorer VIII were obtained. Actually, two interpretations of the direct measurements were possible. They were: (1) the mass distribution curve obtained from the direct measurements departed significantly from those obtained by extrapolating results from meteor observations, or (2) the direct measurements were indicating the presence of a geocentric concentration of dust particles. Although the first interpretation seemed to be in better agreement with the early data, quantitative arguments for its validity were not possible until the data sample was obtained with the microphone system on Explorer VIII.

A segmented approximation to the cumulative mass distribution curve (fig. 2) is shown, together with several model distributions and observational results from the studies of meteors, in fig. 4. The cumulative influx rates obtained by the various observational methods are plotted as a function of particle mass or visual magnitude, with the approximate radiation pressure limits for selected values of mass density being given as an auxillary abscissa.

Visual magnitude has been introduced as an abscissa because the results from meteor observations can be placed on a mass distribution curve only within the limits set by the uncertainty (~ 200) in the mass to magnitude relationship. Visual magnitude is related to particle mass in fig. 4 by assuming that the luminosity of meteors with a given speed depends linearly on the mass of the meteoroid and that a meteoroid with a mass of 25 g and a speed of 28 km sec^{-1} will produce a meteor of zero visual magnitude [35]. Use of a mass density greater than the value of 0.05 g cm^{-3} used by Whipple [35] shifts the influx rate for meteoroids of a given mass toward a lower value.

The distribution curves for meteors given by Whipple [35], McKinley [40], and Hawkins and Upton [37] are shown in fig. 4 with influx rate plotted as a function of visual magnitude. A mass distribution given by Hawkins [41] for asteroids and fireballs is also included. The distribution given by Watson [31] is plotted in terms of particle mass in order that the difference between the Watson and Whipple distributions can be used to illustrate the uncertainty in the influx rate of meteorids of a given mass resulting from the poorly known mass to magnitude relationship for meteors. The direct measurements are not affected by this uncertainty. The uncertainties encountered in placing the direct measurements on a cumulative mass distribution curve are about two orders of magnitude smaller than for meteoroids.

As is shown in fig. 4, the mass distribution curve obtained from the direct measurements departs markedly from those obtained by extrapolating results from meteor observations. It is evident that the constant mass per magnitude relationship does not hold for dust particles in the vicinity of the earth.

There is little evidence that the relationship holds for more than a few magnitudes within any range of particle mass, except possibly for fireballs and asteroids [41]. Therefore, there are no particular reasons for trying to force the direct measurements to fit a constant mass per magnitude curve.

The mass distribution of small dust particles was not known before the data were obtained with Explorer VIII. Several analyses (using best guesses, such as a constant mass per magnitude relationship) for the distribution curve of the direct measurements led to the conclusion that the direct measurements confirmed the existence of a geocentric concentration of dust

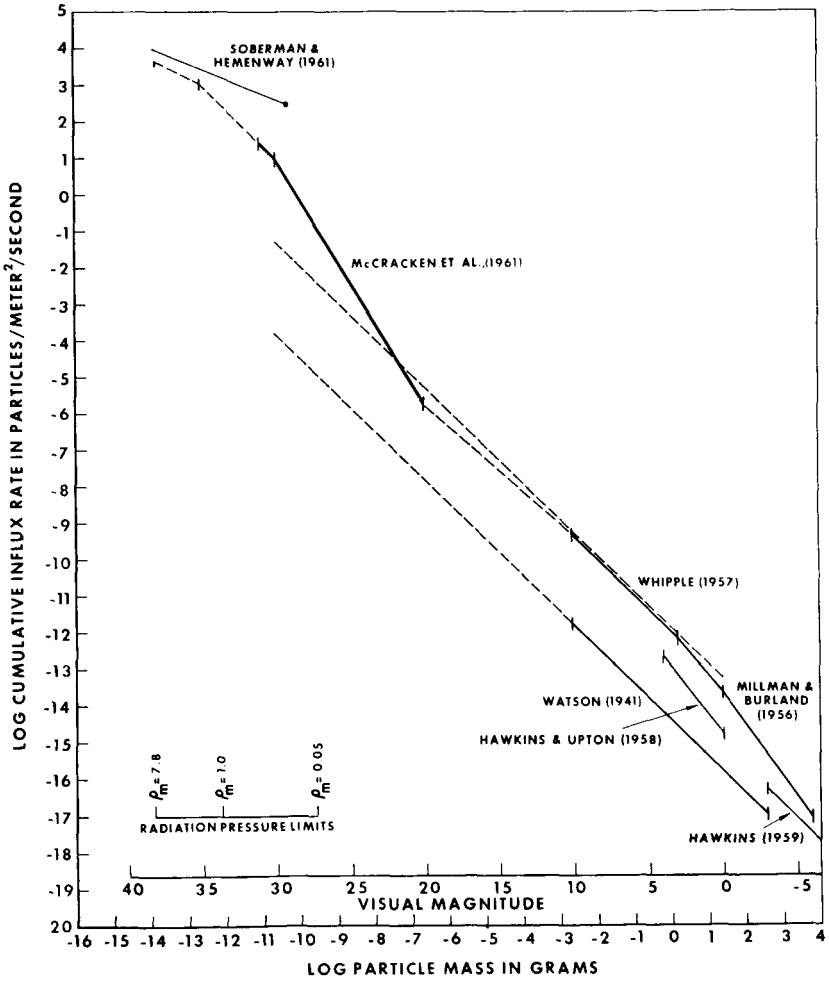

Fig. 4. Segmented cumulative mass distribution curve for omnidirectional influx rates of dust particles and meteoroids.

particles. The results from Explorer VIII and the good agreement of all the other direct measurements with the Explorer VIII data show that these analyses are incorrect, because the measured mass distribution curve differs significantly from those assumed in the analyses.

Some of the more subtle points shown in fig. 4 can be illustrated more clearly by deriving the incremental mass influx curve shown in fig. 5. The incremental mass distribution has been smoothed to remove the effects of using the segmented cumulative mass distribution shown in fig. 4 as a basis for deriving the incremental distribution. The incremental mass influx curve is given in terms of the accretion rate by the earth of dust particles or meteoroids in a given mass range as a function of particle mass or visual magnitude.

The most important conclusion that can be reached on the basis of the distribution curve shown in fig. 5 is that the accretion of interplanetary material by the earth is dominated by the small dust particles. The integrated accretion rate amounts to about 1×10^4 tons per day on the earth.

It must be realized that in both fig. 4 and fig. 5, the distribution curves for particles with masses less than about 10^{-11} g are more uncertain than

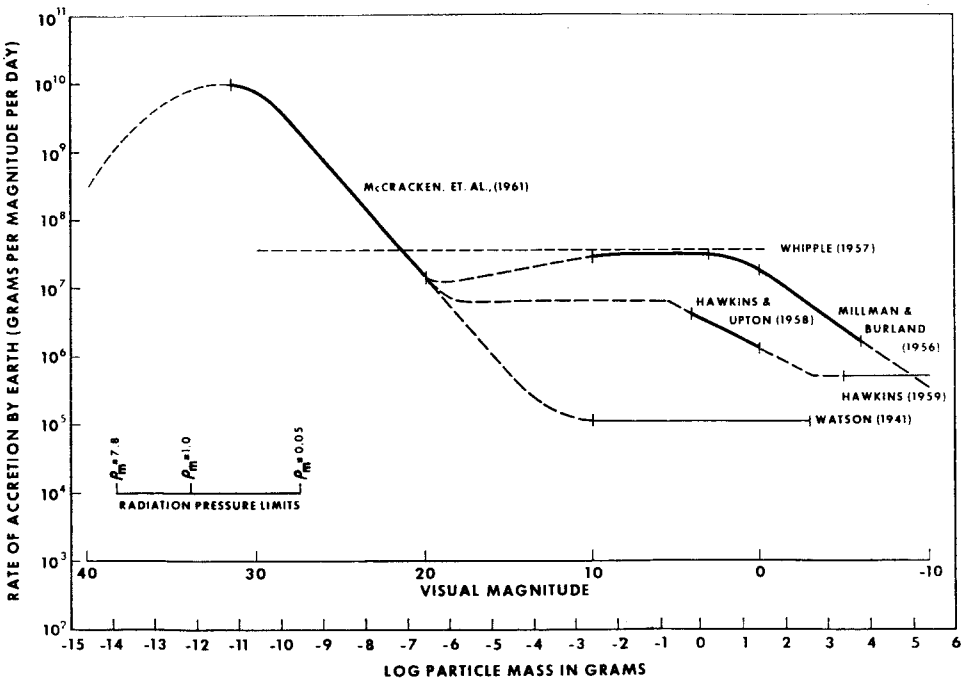

Fig. 5. Incremental mass influx curve for interplanetary material accreted by the earth.

the segments of the curves derived from microphone results. Dust particles with masses less than about 10^{-9} g are subject to the perturbative effects of radiation pressure. The shape of the distribution curves in the submicron range of particle size depends critically on the locations of the sources, on the distribution of orbits, and on the mass densities of the dust particles.

Gallagher and Eshleman [42] have found that the influx rates of faint radar meteors show large fluctuations with time. The observed grouping of radiants suggests that the faint radar meteors are members of "sporadic showers" rather than dispersed members of major meteor streams. Large fluctuations in the influx rate also seem to be the rule rather than the exception in the case of direct measurements. Dubin [7, 8] has reported on the large fluctuations observed with Explorer I. Large fluctuations in the influx rate have also been reported for Vanguard III [43, 44] and for Sputnik III [16, 18], although there is still some question about the latter oase. The fluctuations in influx rate observed on Vanguard III and Explorer VIII are presently under analysis. It appears, on the basis of both the direct measurements and the data for faint radar meteors, that the dust particles are not nearly so uniformly distributed as are the sporadic meteoroids.

The interplanetary dust particle event detected by Explorer I on 2–3 February and shown in fig. 6 may be evidence of a "sporadic shower" of

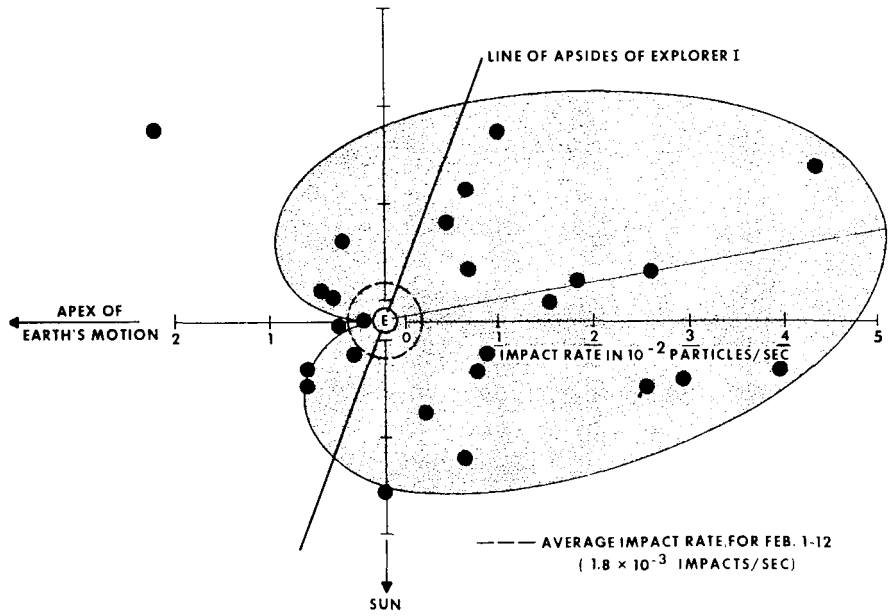

Fig. 6. Impact rates during the February 1958 interplanetary dust particle event.

small dust particles, since it bears no relationship to a known meteor shower. The large increases in influx rate that occurred during the 16–18 November interplanetary dust particle event observed with Vanguard III are shown in fig. 7. The coincidence in time with the expected annual return of the Leonid meteor shower suggests that large numbers of small dust particles are

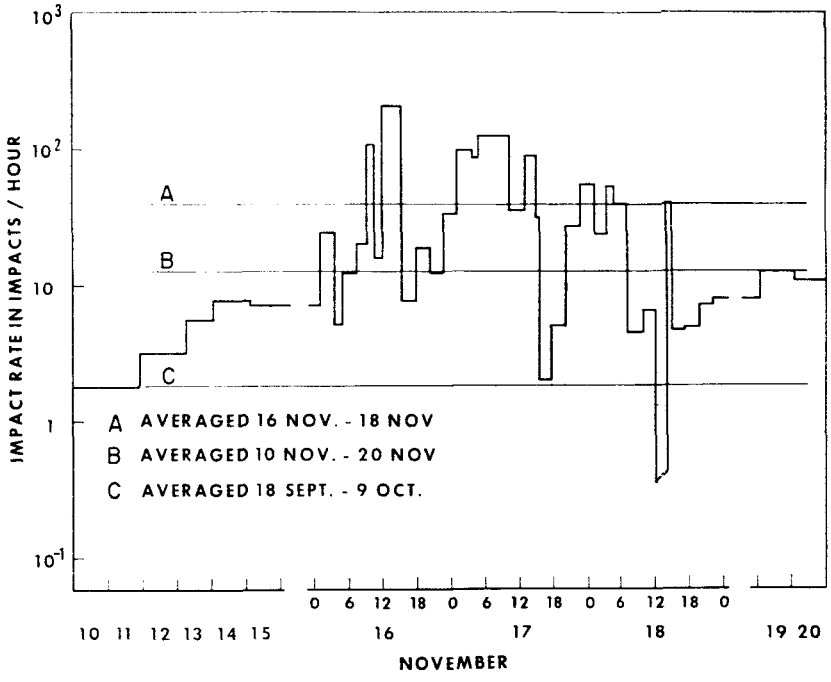

Fig. 7. Impact rates during the November 1959 interplanetary dust particle event.

being generated in the Leonid meteor stream. The microphone system was almost omnidirectional, so it is not possible to establish the radiants of these dust particles. If the particles did belong to the Leonid stream, the difficulty encountered in keeping such dust particles in the stream for one orbital period would require the small particles to have been observed soon after being released from larger meteoroids which were approaching perihelion passage.

Eshleman [45] has reported that the influx rates of the faint radar meteors seem to increase rather than decrease as the limiting sensitivity of the equipment is approached. This increase in influx rate may be evidence that the distribution curve obtained from the direct measurements can be extrapolated to join onto a distribution curve for meteoroids at a visual magnitude of about 15 (see fig. 4 or 5).

7. Comparison of direct measurements with results from observations of the zodiacal light and solar corona

Photometric observations of the zodiacal light and the solar corona have yielded a considerable amount of information about the material in the zodiacal cloud that surrounds the sun. The results obtained by analyzing the observations are generally expressed in terms of the spatial densities and variations in spatial density of electrons and dust particles with distance from the sun. Incremental size distributions for the dust particles are also obtained in the analyses.

Direct measurements of the spatial density, mass distribution, and selected physical parameters of interplanetary dust particles have not yet been obtained for regions of space removed from the earth-moon system. The spatial densities and size distributions of dust particles inferred from photometric studies of the zodiacal light and solar corona presently represent the only available information about small dust particles in the zodiacal cloud.

Comparisons between the direct measurements and the results from the observations of the zodiacal light and the solar corona represent the only means of determining whether the available direct measurements obtained near the earth are also characteristic of interplanetary space. Dubin and McCracken [46] have compared the direct measurements with the results obtained in investigations of the zodiacal light and solar corona by van de Hulst [47], Allen [48], Elsässer [49], and Ingham and Blackwell [50]. It was found that if the results obtained by Ingham and Blackwell were taken as representative of interplanetary space, a spatial density near the earth at least three orders of magnitude higher than for interplanetary space must be introduced in order to remove the discrepancy. There is such a lack of agreement among the results from the various investigations of the photometric observations that the comparisons of results obtained by the two observational techniques are, at best, of a qualitative nature.

8. Conclusions

The direct measurements obtained with the microphone system on Explorer VIII have provided a basis for analyzing all the available direct measurements of interplanetary dust particles. An average cumulative mass distribution curve, subject only to very minor uncertainties, has been established for dust particles in the vicinity of the earth. This average distribution is valid, within an order of magnitude or less, for particles with masses between 10^{-13} g and 10^{-6} g. The irregular shape of the distribution curve.

precludes the possibility of writing its equation in a simple analytical form.

The mass distribution curve obtained from the direct measurements differs markedly from those expected on the basis of extrapolations of results from meteor observations. As a consequence of this difference, the accretion of interplanetary matter by the earth may be said to be dominated by small dust particles with masses less than about 10^{-6} g. A conservative estimate of the accretion rate is 10^4 tons per day on the earth.

The influx rates obtained from the direct measurements undergo large fluctuations and, in one case, show a correlation in time with the expected annual return of a major meteor shower. These fluctuations suggest that the dust particles are not predominantly in long-lived orbits about the earth.

Comparisons of the direct measurements for the vicinity of the earth with the spatial densities of dust particles inferred from photometric studies of the zodiacal light and the solar corona for interplanetary space show discrepancies. These discrepancies may be as large as 10^4; however, such comparisons are uncertain because of the large discrepancies among the photometric data.

The available direct measurements are not sufficient to define either an average geocentric speed or an average mass density. The direct measurements encompass a range of particle mass that extends well past the radiation pressure limits for particles in heliocentric orbits with mass densities of 0.05 g cm^{-3}. Mass densities of approximately 1 g cm^{-3} seem more reasonable for the direct measurements range of particle size. In view of the uncertainties concerning the probable origin (or origins) of particles, the distribution of orbits, and the mass densities of dust particles of micron-size, it does not seem wise to extrapolate results from the meteoroidal range of particle size to the smaller sizes of dust particles.

The various departures of the direct measurements from what has been expected on the basis of other methods of observation demonstrate the feasibility of using the direct measurements technique to study material in the zodiacal cloud. Appropriate direct measurements will serve to answer most of the questions that have been left unanswered in this analysis and represent an important means of determining the predominant source of the dust particles that are observed in the vicinity of the earth.

References

1. M. C. Kells *et al.*, Proc. of Third Symposium on Hypervelocity, Vol. I, Chicago, October 1958, ed. F. Genevese (Chicago, Armour Research Foundation 1959) 361
2. K. P. Stanyukovich, Artificial Earth Satellites, Vol. 4 (New York, Plenum Press 1961) 292

3. M. A. Lavrentyev, Artificial Earth Satellites, Vol. 3, (New York, Plenum Press 1961) 85
4. C. W. McCracken, W. M. Alexander and M. Dubin, Nature 192 (1961) 441
5. C. W. McCracken and W. M. Alexander, 1961, The Distribution of Small Interplanetary Dust Particles in the Vicinity of Earth, Paper presented at the International Symposium on the Astronomy and Physics of Meteors, Cambridge (to be published in 1962)
6. M. Dubin, Space Research I, ed. H. K. Kallmann-Bijl (Amsterdam, North-Holland Publishing Company 1960) 1042
7. M. Dubin, Plan. and Sp. Sci. 2 (1960) 121
8. M. Dubin, J. Geophys. Res. 66 (1961) 2592
9. M. Dubin, W. M. Alexander and O. E. Berg, Cosmic Dust Showers by Direct Measurements, Paper presented at the International Symposium on the Astronomy and Physics of Meteors, Cambridge 1961 (to be published in 1962)
10. W. M. Alexander and O. E. Berg, Microparticle Hypervelocity Impacts from Ranger I, Paper presented at the Fifth Hypervelocity Symposium, Denver 1961 (to be published)
11. R. S. Soberman and L. Della Lucca, G.R.D. Res. Note No. 72 (AFCRL, Bedford, Mass. 1961)
12. H. E. LaGow, D. H. Schaefer and J. C. Schaffert, 1958, Micrometeorite Impact Measurements on a 20″ Diameter Sphere at 700 to 2500 Kilometers Altitude, Paper presented at the CSAGI meeting of the IGY, Moscow
13. H. E. LaGow (private communication)
14. C. W. McCracken, An Analysis of Rocket and Earth Satellite Measurements of Micrometeoric Influx, M.S. Thesis (Oklahoma State University, Stillwater 1959)
15. R. F. Buck, 1960, Final Report, Contract No. AF 19(604)–1908 with Oklahoma State University
16. T. N. Nazarova, Space Research I, ed. K. H. Kallmann-Bijl (Amsterdam, North-Holland Publishing Company 1960) 1059
17. T. N. Nazarova, Rocket and Satellite Meteoric Dust Investigations, Paper presented at the XIII International Astronautical Congress, Washington 1961
18. T. N. Nazarova, Results of Exploring Meteoric Matter with Instrumentation of Sputnik III and Space Probes, Paper presented at the XI International Astronautical Congress, Stockholm 1960
19. O. E. Berg and L. H. Meredith, J. Geophys. Res. 61 (1956) 751
20. J. E. Friichtenicht, Experiments with a Two Million Volt Electrostatic Generator, Paper presented at the Fifth Hypervelocity Symposium, Denver 1961
21. J. F. Lovering, Plan. and Sp. Sci. 2 (1959) 75
22. R. S. Soberman, C. L. Hemenway, *et al.*, 1961, G.R.D. Res. Note No. 71 (AFCRL, Bedford, Mass.)
23. E. R. Manring, Plan. and Sp. Sci. 1 (1959) 27
24. H. A. Cohen, A. Corman and M. Dubin, Proc. of the Third Symposium on Hypervelocity Impact, Chicago, October 1958 (Chicago, Armour Research Foundation 1958)
25. H. E. LaGow, L. Secretan and J. Giuliani, Experiments for Satellite Environmental Measurements, Paper presented at the CSAGI meeting of the IGY, Washington 1957
26. H. E. LaGow and L. Secretan, The Micrometeorite Penetration Experiment, NASA TN D–608
27. E. H. Davison and P. C. Winslow Jr., Aerospace Engineering 21 (1962) 24

28. E. H. Davison and P. C. Winslow Jr., Space Debris Hazard Evaluation, NASA TN D–1105 1961
29. J. L. Summers, Investigation of High-Speed Impact: Regions of Impact and Impact at Oblique Angles, NASA TN D–94 1959
30. C. R. Nysmith and J. L. Summers, Preliminary Investigation of Impact on Multiple-Sheet Structures and an Evaluation of the Meteoroid Hazard to Space Vehicles, NASA TN D–1039 1961
31. F. G. Watson, Between the Planets (Philadelphia, The Blakiston Company 1941)
32. G. Grimminger, J. App. Phys. **19** (1948) 947
33. F. L. Whipple, Physics and Medicine of the Upper Atmosphere, ed. Clayton S. White and Otis O. Benson Jr. (Albuquerque, University of New Mexico Press 1952) 137
34. F. L. Whipple, International Astronomical Union Symposium, Number 4: Radio Astronomy, ed. H. C. van de Hulst (New York, Cambridge University Press 1957) 375
35. F. L. Whipple, Proc. of the VIII International Astronautical Congress, Barcelona, October 1957 (Vienna, Springer Verlag 1958)
36. P. M. Millman and M. S. Burland, Magnitude Distribution of Visual Meteors, Paper given at the 96th meeting of the American Astronomical Society, New York 1956
37. G. S. Hawkins and E. K. L. Upton, Ap. J. **128** (1958) 727
38. M. Dubin, Direct Measurement of Meteoric Dust Using Rockets and Satellites, Paper presented at the 10th General Assembly of the International Astronomical Union, Moscow 1958
39. T. N. Nazarova, Rocket and Satellite Investigation of Methods — Study of Meteors on Rockets and Satellites, Paper presented at the 10th General Assembly of the International Astronomical Union, Moscow 1958
40. D. W. R. McKinley, Meteor Science and Engineering (New York, McGraw-Hill Book Company, Inc. 1961)
41. G. S. Hawkins, A. J. **64** (1959) 450
42. P. B. Gallagher and V. R. Eshleman, J. Geophys. Res. **65** (1960) 1846
43. H. E. LaGow and W. M. Alexander, Space Research I, ed. H. K. Kallmann-Bijl (Amsterdam, North-Holland Publishing Company 1960) 1033
44. W. M. Alexander, C. W. McCracken and H. E. LaGow, J. Geophys. Res. **66** (1961) 3970
45. V. R. Eshleman, Radar Rate Measurements on Very Small Meteors, Paper presented at the Symposium on Small Meteoritic Particles in the Earth's Neighborhood, 110th meeting of the the American Astronomical Society, Cambridge 1962
46. M. Dubin and C. W. McCracken, Measurements of Distributions of Interplanetary Dust, Paper presented at the Symposium on Small Meteoritic Particles in the Earth's Neighborhood, 110th meeting of the American Astronomical Society, Cambridge, 1962 (to be published)
47. H. C. van de Hulst, Ap. J. **105** (1947) 47
48. C. W. Allen, Mon. Not. R.A.S. **106** (1946) 137
49. H. Elsässer, Zs. F. Ap. **37** (1954) 114
50. M. F. Ingham, Observations of the Zodiacal Light from a Very High Altitude Station IV (See also the three preceding papers, pp. 113–155, by D. E. Blackwell and M. F. Ingham), Mon. Not. R.A.S. **122** (1961) 157